PASJ: Publ. Astron. Soc. Japan **53**, 243–250, 2001 April 25

Low-Temperature Optical Properties of Silicate Particles in the Far-Infrared Region

Hiroki CHIHARA,[1,2] Chiyoe KOIKE,[2] and Akira TSUCHIYAMA[1]
[1]*Department of Earth and Space Science, Osaka University, 1-1 Machikaneyama, Toyonaka, Osaka 560-0043*
chi@ess.sci.osaka-u.ac.jp
[2]*Kyoto Pharmaceutical University, Misasagi, Yamashina, Kyoto 607-8412*

(Received 2000 July 23; accepted 2000 December 20)

Abstract

The far-infrared absorption spectra of crystalline circumstellar dust analogues (orthoenstatite, clinoenstatite, diopside, and forsterite) were measured at room temperature (295 K) and liquid-helium temperature (4.2 K). The wavelength ranges of the measurements were 20–80 μm and 30–80 μm at 295 K and 4.2 K, respectively. The absorption bands were detected very clearly not only at room temperature, but also at liquid-helium temperature. The temperature effects were clearly observed at liquid-helium temperature, such as (1) an increase in the spectral index of the continuum, (2) an enhancement in the absorption band strength, (3) a decrease in the band width, and (4) the absorption peaks of all bands of all samples shifted toward a shorter wavelength. These results suggest that a reconsideration of the identification should be required for some absorption bands which have been recognized as unidentified bands because of a disagreement in the peak position between the observed data and the laboratory data obtained at room temperature. Our experimental data can be obtained from the web-site (http://www.kyoto-phu.ac.jp/labo/butsuri/).

Key words: crystalline silicate — ISM: dust, extinction — ISM: lines and bands — laboratory experiment — line: profiles

1. Introduction

Laboratory measurements of the infrared absorption spectra of the cosmic dust analogue are essential for the correct interpretation of the observational data. Almost all of the laboratory spectra published in the astronomical context, however, were usually measured at room temperature. Although the temperature effect of the optical behavior of the crystalline cosmic dust analogue was predicted from the viewpoint of solid-state physics, extensive experimental studies on the low-temperature spectra of the materials relevant to astrophysics are rarely to be found in the literature. Some experimental work on this subject has been carried out from an astronomical perspective. Day (1976) measured the mid-infrared spectra of crystalline forsterite and pyroxene at room temperature and 80 K. He reported an enhancement of the spectral features at 80 K, such that the intensity and sharpness of the absorption bands increased, and that some peaks shifted toward shorter wavelengths. More recently, Henning and Mutschke (1997) carried out measurements of the reflectance and absorption spectra for crystalline and amorphous silicate and other cosmic dust analogues at low temperatures. They reported that the vibrational bands of the reflectance spectra showed a sharpening and strengthening with decreasing temperature. However, the temperature effect was weak for the absorption spectra, especially for crystalline silicate, for which a larger effect should be expected from a theoretical point of view. They expressed their result for crystalline silicate that the effect was surprisingly weak. Koike and Shibai (1998) reported that the intensity of the mid-infrared absorption bands of olivine and pyroxene increased at about 110 K. They also measured the spectra of other cosmic dust analogues at liquid-helium temperature in the far-infrared region, but the temperature effects did not appear clearly, except for amorphous carbon. Mennella et al. (1998) also investigated the temperature effects on the spectral features of carbonaceous materials, crystalline silicate, and amorphous silicate from the 20 μm to millimeter region in the temperature range 295–24 K. They reported that the absorption bands of crystalline silicates shifted to shorter wavelengths at low temperatures and the fact that the far-infrared emissivities of all the samples decreased with decreasing temperature. Their measurements showed that the temperature effects are more remarkable for amorphous materials than for crystalline ones. Bowey et al. (2000) discussed, in their recent report, the spectral variation of crystalline silicates at 1.5 K and 295 K. According to them, a band shift of forsterite was seen clearly; however, for pyroxene and hydrous silicates, the shift was more complicated, since the neighboring bands were shifted by different amounts. These experimental studies revealed that the temperature significantly affects the optical properties of the cosmic dust analogue. In these previous studies, however, no quantitative discussion on the variation in the individual absorption bands was satisfactorily given, because of uncertainties due to the particle agglomeration and the low spectral-resolution of the measurements. In the present work, we try to quantitatively investigate the temperature effects on the far-infrared absorption spectra of pure and high-quality synthetic crystalline silicates with a Fourier transform spectrometer having high resolution.

Table 1. Samples.

Sample	Chemical formula	Synthetic method	Reference
Orthoenstatite	$MgSiO_3$	Flux method	Tachibana (2000)
Clinoenstatite	$MgSiO_3$	Flux method and reheating	Tachibana (2000)
Diopside	$CaMgSi_2O_6$	CZ method	Takei, Miura, and Morioka (1982)
Forsterite	Mg_2SiO_4	CZ method	Takei and Kobayashi (1974)

2. Experiment

2.1. *Sample Preparation*

The measured samples were Mg-bearing silicates: orthoenstatite ($MgSiO_3$) and clinoenstatite[3] ($MgSiO_3$) (Tachibana 2000), diopside ($CaMgSi_2O_6$) (Takei et al. 1982) and forsterite (Mg_2SiO_4) (Takei, Kobayashi 1974). All of the samples were synthesized by the appropriate synthetic methods summarized in table 1. Orthoenstatite was synthesized by the flux method. In order to obtain clinoenstatite, orthoenstatite was reheated above the protoenstatite–orthoenstatite phase transition point (1258 K) for several hours in air, and then quenched in water. The resulting material was clinoenstatite. In the flux method, the components of the material are dissolved in a high-temperature solvent. The single crystals are deposited from a high-temperature supersaturated solution, while the temperature of the solution decreases. The solvent is called a flux, which is selected depending on the crystals. In this work we used a Li_2O–MoO_3–V_2O_5 flux to deposit orthoenstatite. Diopside and forsterite were synthesized by the Czochralski (CZ) method. The CZ method is widely known as a commercial technique for growing bulk single crystals of semiconductors, oxides, and metals. In the CZ method, a seed crystal is dipped into a melt of the materials to be grown, and then pulled slowly. The seed is rotated at the same time to control the shape of the crystal and to homogenize the quality of the crystal.

The purity of the samples was 99% or more for ortho- and clinoenstatite, and more than 99.9% for diopside and forsterite. In general, the enstatite synthesized with the flux method contained a small amount of the materials of flux as impurities. Tachibana (2000) reported that the amount of impurities in the orthoenstatite were 0.18 weight % for V_2O_5, 0.17 weight % for Li_2O, and less than 0.1 weight % for MoO_3. The amount of impurities to this extent will not affect the absorption spectra.

The bulk single crystals were crushed and ground in an agate motor for 1–2 hr. These fine particles having sized less than 1 μm were dispersed and embedded in low-density polyethylene at the proper concentration. A blank polyethylene pellet was measured as a reference at both room and liquid-helium temperature in this work.

[3] Clinoenstatite is the metastable phase of orthoenstatite. It is converted via a phase transition from protoenstatites, which is the higher temperature phase of orthoenstatite. Despite the identical chemical composition of orthoenstatite and clinoenstatite, the crystal structure is not the same. That is, the crystal system is orthorhombic for orthoenstatite and monoclinic for clinoenstatite.

2.2. *Measurement Procedures*

The absorption spectra at room temperature were obtained with a Jasco FT/IR-350 spectrometer (Kyoto Pharmaceutical University) with a resolution of 0.5 cm^{-1}. In order to avoid the absorption of water vapor in the far-infrared region, the sample chamber was purged by dry air. Measurements at liquid-helium temperature were carried out with a Bomen DA8 FT spectrometer at the Institute of Space and Astronautical Science (ISAS) with a resolution of 0.1 cm^{-1}. The detector of the latter spectrometer was a silicon bolometer which works at liquid-helium temperature. The detector and the sample holder were located in a cryostat insulated with two-folded dewars (Infrared Labo. HDL-5). The sample holder was made of brass, and six pellets could be mounted at the same time. The blank polyethylene pellet was measured as the reference. The spectral change of polyethylene was reported by Brandli and Sievers (1972). In the wavelength range of this work, the absorption bands existed at 114.7 cm^{-1} and 229.8 cm^{-1} at 295 K. These bands shifted to 113.0 cm^{-1} and 234.5 cm^{-1} at 4 K. Nevertheless, it should be considered that these spectral changes of the polyethylene did not affect the results of these measurements, because the blank polyethylene pellet was also mounted in the cryostat.

In the cryostat the sample holder and the detector were cooled by liquid helium through thermal conduction. The cooling started when the pressure inside the cryostat decreased below 1×10^{-6} Torr; the two-folded dewars were filled with liquid N_2. After about 6 hr, the liquid N_2 was removed only from the inner dewar, and liquid helium was put into the inner dewar. The measurements were started after about 1 hr from the first injection of liquid helium into the inner dewar. Unfortunately, a thermometer could not be attached to the sample fingers. Nevertheless, it is considered that thermal equilibrium in the cryostat was achieved, since the signals of the detector did not change practically less than 1% while the measurements were being carried out for about 8 hr.

The purpose of this work was, on one hand, to detect any temperature effects on the spectral features and, on the other hand, to derive precise absorption profiles of crystalline silicates at cryogenic temperature. Therefore, in this work we used a higher resolution (0.1 cm^{-1}) at liquid-helium temperature in order to determine the peak position, strength, and width of the absorption band exactly. Here, it should be noted that an enhancement in the strength and the sharpness was also generally produced by an improvement of the spectral resolution of the spectrometer. Indeed, as a result of our preliminary measurement, the spectra which were obtained at two different resolutions (0.5 cm^{-1} and 0.1 cm^{-1}) at liquid-helium temperature showed that the peak strength increased by a factor of

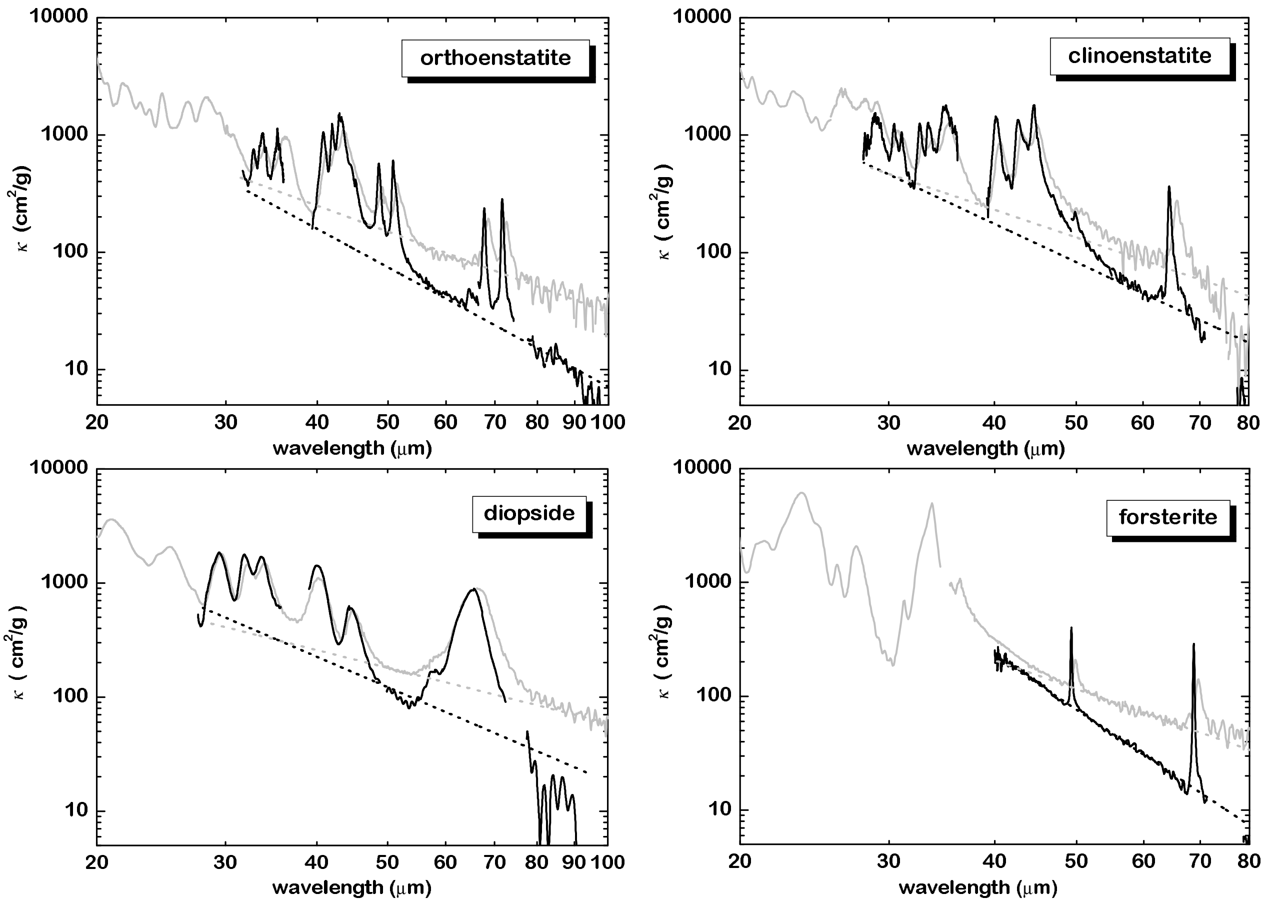

Fig. 1. Mass-absorption coefficient, κ. The solid curves and the gray curves show the values of κ at liquid-helium temperature and room temperature, respectively. The continuums are superposed with dashed lines.

approximately 1.1 at higher resolution for the 40 and 70 μm bands of orthoenstatite, for example. However, the effect for the band width was weak, because the band width was actually larger than the resolution of the spectrometer. In order to correct the resolution effect, the data were convolved by a slit function; the width of the function corresponded to 0.5 cm^{-1}. As a result, the decreasing of the peak strength and the broadening of the band widths were emulated. The peak strength of the convolved data were decreased by about 10% on average, compared to those of the raw data. However, the change in the band width was very small, since the width of the absorption bands was much wider than the resolution of the spectrometer.

3. Results

In figure 1 the mass absorption spectra of all samples at room temperature and liquid helium temperature are plotted. The mass absorption coefficients, κ, was defined from the relation

$$\kappa = \frac{S}{M} \log\left(\frac{1/T}{1/T_{\mathrm{R}}}\right). \tag{1}$$

Here, S, M, T and T_{R} are the cross section of a pellet, the mass of a pellet, the transmittance of a sample and that of a blank pellet, respectively. For measurements at liquid-helium temperature, large instrumental noise and vapor absorptions occurred in the 34–38 μm and 74–78 μm regions. Therefore, the data in these regions were eliminated from the plots. For forsterite, the signals were saturated in the region below 40 μm at liquid-helium temperature. From these plots, it is obvious that the absorption features change drastically at liquid-helium temperature. The transmittance in the far-infrared region at liquid-helium temperature increased significantly. In order to estimate the steepness of the continuum in the far infrared region, the underlying continuums were fitted in the range about 30–80 μm with a power law of

$$\kappa = c\,\lambda^{-\beta}. \tag{2}$$

The constant, c, and the spectral index, β, at room and liquid-helium temperature are given in table 2. The index β increased at liquid-helium temperature by factors of 1.5, 1.4, 1.7, and 1.9 for orthoenstatite, clinoenstatite, diopside, and forsterite, respectively. Mennella et al. (1998) also reported a change in the spectral index of crystalline and amorphous silicates. According to them, the value of β of crystalline forsterite was 2.04 and 2.32 at 295 K and 24 K, respectively. Our results, however, gave a β of 2.6 and 5.0 at room temperature and liquid-helium temperature. There are two possible reasons for the discrepancies. The first is due to the different ranges for estimating β. It should be noted that Mennella et al. (1998) estimated β over a wide range from 100 μm to 2 mm. In

Table 3. Parameters of the individual peak characters.

Species	λ_{RT} [μm]	λ_{LT} [μm]	$\Delta\lambda$ [μm]	$\frac{\kappa_{LT}}{\kappa_{RT}}$	$\frac{\kappa^{cs}_{LT}}{\kappa^{cs}_{RT}}$	$\frac{I_{LT}}{I_{RT}}$	$FWHM_{RT}$ [μm]	$FWHM_{LT}$ [μm]	$\frac{FWHM_{LT}}{FWHM_{RT}}$
Orthoenstatite	33.2	32.8	−0.4	1.2	1.6	1.1	0.73	0.36	0.5
	33.9	33.6	−0.3	1.3	1.7	1.8	0.73	0.68	0.9
	36.1	35.3	−0.8	1.2	1.4	0.5	1.30	0.69	0.5
	41.2	40.8	−0.5	1.5	1.9	2.1	0.56	0.59	1.1
	42.4	41.9	−0.5	1.6	2.0	1.3	0.66	0.28	0.4
	43.5	43.2	−0.3	1.3	1.5	1.2	1.92	1.66	0.9
	49.1	48.6	−0.6	1.6	2.4	1.7	0.87	0.54	0.6
	51.4	50.8	−0.6	1.6	2.2	1.3	1.18	0.68	0.6
	68.5	67.7	−0.8	1.2	1.7	0.9	1.25	0.63	0.5
	72.6	71.6	−1.0	1.6	2.2	1.1	1.27	0.59	0.5
Clinoenstatite	29.1	28.9	−0.2	0.8	0.7	0.7	0.95	0.90	1.0
	30.7	30.4	−0.3	1.1	1.2	1.0	0.45	0.29	0.7
	31.2	31.1	−0.2	1.1	1.3	1.0	0.44	0.25	0.6
	32.9	32.6	−0.3	1.3	1.5	1.1	0.45	0.27	0.6
	33.8	33.4	−0.4	1.4	1.6	1.1	0.67	0.37	0.6
	35.3	35.1	−0.3	1.4	1.6	1.7	1.35	1.46	1.1
	40.6	40.2	−0.4	1.6	2.0	1.8	0.80	0.70	0.9
	43.1	42.7	−0.5	1.3	1.4	1.6	0.92	0.88	1.0
	45.0	44.6	−0.4	1.5	1.6	0.8	2.07	1.08	0.5
	65.8	64.4	−1.4	1.3	1.6	0.7	1.39	0.55	0.4
Diopside	29.5	29.4	−0.1	1.0	1.0	0.9	1.12	1.06	0.9
	32.1	31.8	−0.3	1.2	1.2	1.2	0.92	0.83	0.9
	33.9	33.6	−0.3	1.1	1.1	1.1	1.61	1.51	0.9
	40.2	40.0	−0.2	1.3	1.4	1.4	2.06	1.97	1.0
	44.7	44.5	−0.2	1.1	1.2	1.4	1.32	1.38	1.0
	66.2	65.3	−0.9	1.0	1.0	0.8	5.21	4.62	0.9
Forsterite	49.8	49.3	−0.5	1.9	3.4	1.0	0.59	0.17	0.3
	69.7	68.8	−0.9	2.0	2.9	0.7	1.34	0.27	0.2

Table 2. Parameters of underlying continnum.

	295 K		4 K	
	c	β	c	β
Orthoenstatite	1.1×10^6	2.3	4.1×10^7	3.4
Clinoenstatite	1.9×10^6	2.4	4.3×10^7	3.4
Diopside	9.6×10^4	1.6	5.7×10^6	2.7
Forsterite	3.1×10^6	2.6	2.1×10^{10}	5.0

contrast, the values of β in this work were estimated over very narrow ranges below 100 μm. The second reason is the uncertainty due to particle agglomeration. The value of β is sensitive to particle agglomeration in the matrix, especially in the far-infrared region. In general, β has a tendency to decrease as the degree of agglomeration increases (Koike, Shibai 1994). It is also recognized that the strength and sharpness of the peaks of the absorption bands increased exceedingly at liquid-helium temperature. Table 3 summarizes the parameters of the spectral features.

To analyse the intrinsic features of the individual absorption bands in detail, the underlying continuum was subtracted from the raw spectra. For these residual spectra, each band was fitted with a Lorentzian,

$$\kappa^{cs} = \frac{2I}{\pi}\frac{\omega}{4(\lambda-\lambda_c)^2+\omega^2}. \tag{3}$$

Here, κ^{cs} is the continuum-subtracted mass-absorption coefficient. I, λ_c and ω are the integrated intensity, peak center, and full-width at half-maximum (FWHM), respectively. The continuum-subtracted spectra are plotted in figure 2. The degree of enhancement of the absorption band at liquid-helium temperature can be estimated by the ratio of the mass-absorption coefficients, κ_{LT}/κ_{RT}, the continuum-subtracted mass-absorption coefficients, $\kappa^{cs}_{LT}/\kappa^{cs}_{RT}$, and the integral intensities, I_{LT}/I_{RT}, at liquid-helium temperature to those at room temperature. No significant difference was found in the degree of enhancement between orthoenstatite and clinoenstatite. The largest enhancement was observed in forsterite; the band strengths of the raw spectrum at low temperature were twice as larger as that at room temperature. For diopside, the enhancement was relatively smaller than that of others from the

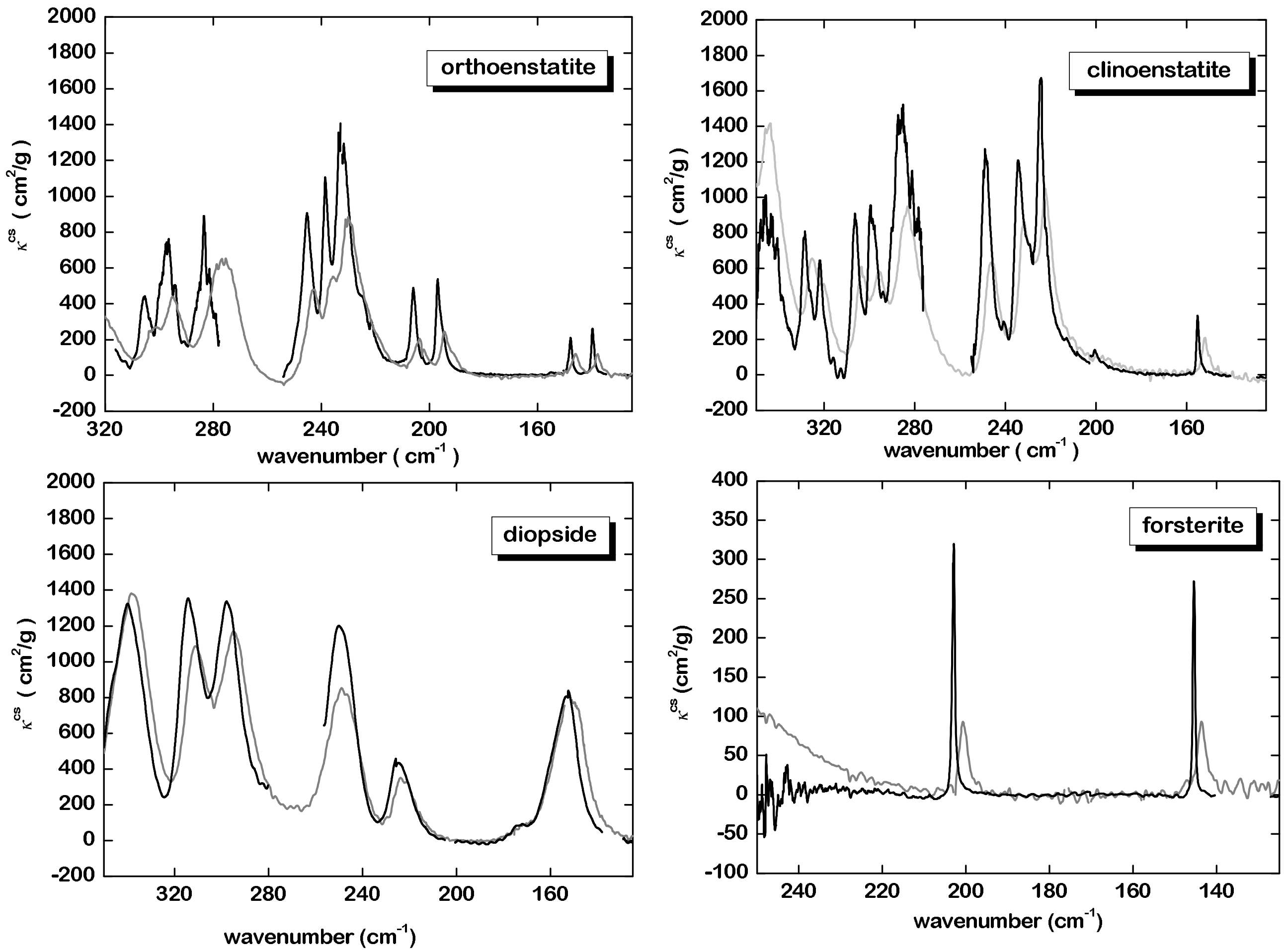

Fig. 2. Continuum-subtracted mass-absorption coefficients, κ^{cs}. The solid curves and gray curves indicate the values of κ^{cs} at liquid-helium temperature and room temperature, respectively.

ratio of κ and κ^{cs}.

The sharpness of the absorption band at helium temperature were estimated with FWHMs. The calculated values of the FWHM are listed in table 3. Except for diopside, a significant decrease in the bandwidth was observed for all samples. The values of the ratios of $FWHM_{LT}/FWHM_{RT}$ at liquid-helium temperature to room temperature were between 0.4 and 1.1 for orthoenstatite and clinoenstatite. The values for forsterite were 0.2 and 0.3.

The peak positions of all absorption bands at liquid-helium temperature shifted toward a shorter wavelength than those at room temperature. Here, the degree of the shift is defined as $\Delta\lambda = \lambda_{RT} - \lambda_{LT}$, where λ_{RT} and λ_{LT} are the peak positions at room temperature and low temperature, respectively. Figure 3a shows the dependence of $\Delta\lambda$ on the wavelength of the peak positions at room temperature, λ_{RT}, for all samples. From the viewpoint of energy, it is convenient to plot this trend for the wavenumber. Figure 3b shows the dependence of $\Delta\nu = \nu_{LT} - \nu_{RT}$ on the wavenumber of the peak positions at room temperature. The definitions of $\Delta\nu$, ν_{LT} and ν_{RT} are the same as the case of $\Delta\lambda$. For forsterite, Mennella et al. (1998) as well as Bowey et al. (2000) measured its absorption coefficient at 24 K and 1.5 K, respectively. In figures 3a and b, their data are superposed. In the results of Mennella et al. (1998), the absorption band at 50 μm was not detected, and the 70 μm band was located at a slightly longer wavelength. The reason of these discrepancies is probably because their measurements were carried out at a lower resolution (4 cm^{-1}) than those of others. The shift of the 36 μm band of orthoenstatite (see table 3) has a larger uncertainty because of the large instrumental noise at 37–41 μm; this point is not plotted in the figure. The shift of the 66 μm band of the clinoenstatite is relatively large. Except for these points, the tendencies of $\Delta\lambda$ for λ_{RT} are very clear for all of the samples. It is also consistent with the results of Mennella et al. (1998) and Bowey et al. (2000) for forsterite. The degree of the peak shift is larger for the absorption band which is located at longer wavelengths; that is, the value of the shift is about 0.9 μm for the 70 μm bands and 0.4 μm for the 40 μm bands. From figure 3b, there is no significant dependence of the peak shift on the energy in the wavenumber scale.

These behaviors of the IR absorption bands at liquid-helium temperature are qualitatively consistent with previous measurements by Mennella et al. (1998) and Bowey et al. (2000). The variation in the band features owing to the temperature effect, however, emerged more distinctly because of the higher spectral resolution.

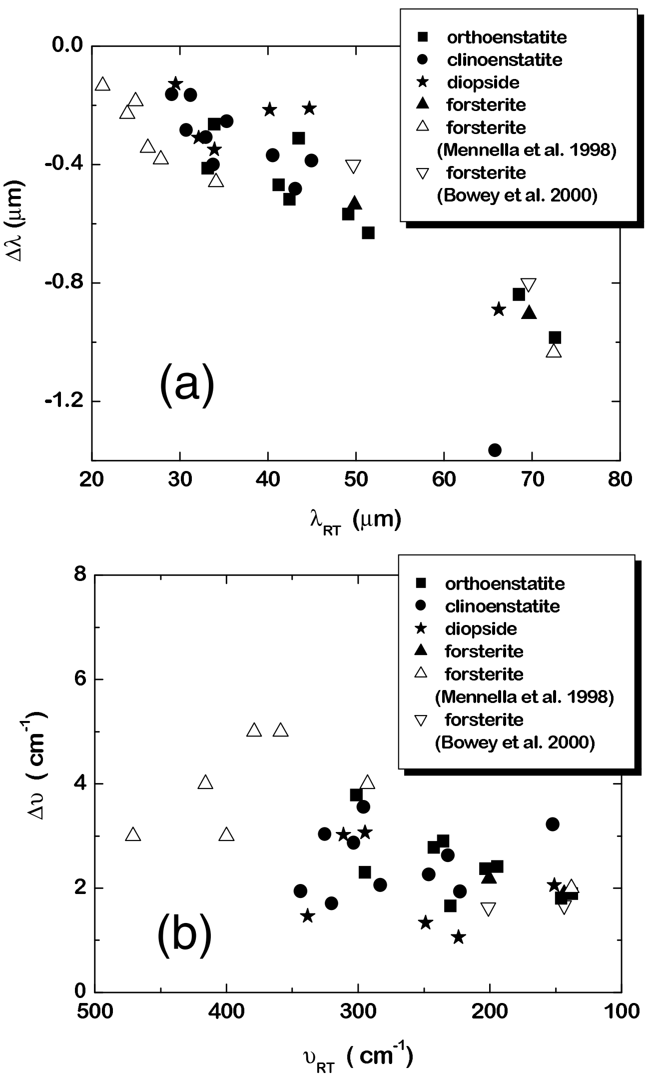

Fig. 3. Continuum-subtracted mass-absorption coefficients, $\kappa^{\rm cs}$. The solid curves and gray curves indicate the values of $\kappa^{\rm cs}$ at liquid-helium temperature and room temperature, respectively.

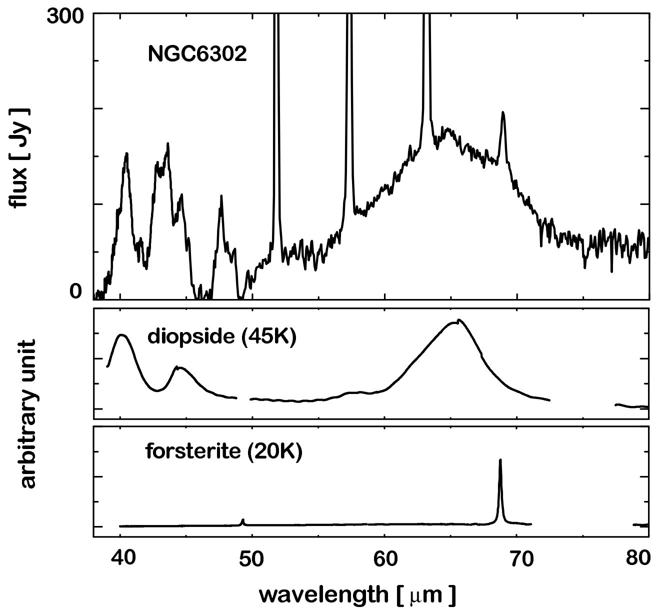

Fig. 4. Comparison between the spectrum of NGC 6302 observed by ISO and the emissivities of diopside at 45 K and forsterite at 20 K. The narrow peak at 52, 57, and 63 μm in the spectrum of NGC 6302 are due to the [O III], [N III] and [O I], respectively (see Pottasch, Beintema 1999).

4. Discussion

4.1. Physical Interpretation of the Temperature Effects

The mechanisms of the temperature effects have been discussed in detail in previous literature (e.g., Tielens, Allamandola 1987; Henning, Mutschke 1997; Mennella et al. 1998). Therefore, we only give an outline here. According to Tielens and Allamandola (1987), the most fundamental origin of the temperature effects is a decrease in the amplitude of the lattice vibration due to a contraction of the crystalline lattice at low temperature. The reduced amplitude of the lattice vibration induces a stronger force constant at low temperatures. Therefore, the potential wall of the lattice vibration becomes deeper and extra energy is required to excite the phonon. As a result, the peaks shift toward shorter wavelengths. However, Henning and Mutschke (1997) explained that the anharmonisty of the potential is a possible origin of the effect. They have pointed out that the temperature should not affect the single-phonon process (a single phonon can be created, the frequency of which corresponds to the energy of an incident photon) significantly, because this process does not depend on the temperature of the material. If the material is thermally excited, however, a further transition may occur between the higher vibrational states by infrared illumination. Consequently, subtle differeces between the potentials cause an anharmonisity of the potential and the shift of the resonance frequency. A decrease in the population of the thermally excited phonons induces an increase in the spectral index and an enhancement in the peak. Tielens and Allamandola (1987) as well as Henning and Mutschke (1997) also explained that the decreasing anharmonisity of a potential of higher order is one reason for the decreasing band width. In general, the width of the absorption band is indicated as the inverse of the lifetime of a phonon in the crystal (e.g. Kudo 1996). At low temperature, the dumping coefficients of the lattice vibration decrease because of a reduction of the population of the thermally excited phonons and a decreasing in the anharmonisity of the higher-order potential. Therefore, the lifetime of a phonon would be longer and the width of the peak would be decreased.

4.2. Implications for the Observational Data

In the present study, the variations in the absorption spectra of the circumstellar dust analogues at liquid-helium temperature were very clear in the far-infrared region. Here, we try to compare the spectrum of NGC 6302 observed by ISO (e.g., Barlow 1998; Lim et al. 1999; Pottasch, Beintema 1999) and the low-temperature laboratory spectra of diopside and forsterite obtained in this work. According to Pottasch and Beintema (1999), the abundances of Mg, Al, Fe, and especially Ca of NGC 6302 are highly depleted in gas phase; these elements may be concentrated in the solid phase. The spectrum of NGC 6302 shows many sharp bands. Some of these bands have been identified with crystalline silicate, such as olivine and pyroxene (Beintema 1998). The 69 μm band may be attributable to crystalline forsterite (Malfait et al. 1998, 1999; Molster 2000). Barlow (1998) pointed out that the carrier of the broad band around 65 μm is crystalline water ice, because of the existence of an incidental band at 44 μm. However, the laboratory spectrum of crystalline water ice shows absorption bands at 44 μm and 62 μm (Smith et al. 1994); also, the relative strength of these bands observed by ISO was different from that derived from laboratory data. They explained these discrepancies on the low characteristic temperature($\sim$ 45 K) of emission in the far-IR region. Koike et al. (2000) argued that the 65 μm band is located at a longer wavelength than that of usual crystalline water ice, and that the width of this band is too broad to be identified with crystalline-water ice. Considering the depletion of calcium and the possibility for the existence of Ca-bearing silicate, they compared the spectrum of NGC 6302 observed by ISO with the laboratory spectrum of diopside measured at room temperature. As a result, they pointed out that the band sequence of the diopside is very similar to that of NGC 6302. They concluded that the extra broadness and the peakshift to a longer wavelength of the 65 μm band may be explained by a mixture of crystalline-water ice and diopside. However, there were some discrepancies concerning the peak positions between the observational data and the laboratory data, especially in the longer wavelength region. They argued that these discrepancies can be resolved with the shift of the peaks, due to a low-temperature effect. In figure 4, the continuum-subtracted spectrum of NGC 6302 observed by ISO and the emissivities of diopside and forsterite multiplied by Planck's function at proper temperatures are shown based on this measurement. The Planck functions were chosen to be the ratio of the relative strength of each band, which is consistent with the observation. The observational peak position of the 69 μm band, which may be attributable to crystalline forsterite, was 1 μm shorter compared with the spectrum at room temperature, though a comparison with the spectrum at liquid-helium temperature gave a good agreement within 0.1 μm. For the 65 μm band in the observational spectrum, the peak positions are almost consistent with the low-temperature spectrum of the diopside. The peak positions of the band in the laboratory spectra are slightly shorter ($\simeq 0.1$ μm) than that of the observed spectrum, because the measurements were carried out at a lower temperature than that expected in the circumstellar environment. The sequence of the band positions of the laboratory spectra are, nevertheless, almost in accord with the observed spectrum. This accordance may support the assumption for the existence of diopside in the region of NGC 6302.

5. Conclusion

The far-infrared absorption spectra on crystalline silicate were measured at room temperature and at liquid-helium temperature. Although the temperature effects of crystalline silicate were predicted from the standpoint of solid-state physics, they were not observed very clearly in measurements of the absorption spectra carried out in the past. In this work, all of the spectral variations at low temperature predicted from solid-state physics were detected distinctly, for the first time, in the absorbance of the crystalline silicate, as follows:

1. Increase of the spectral index of the continuum.
2. Enhancement of the absorption-band strength.
3. Decrease of the band width.
4. Absorption bands shifted toward shorter wavelengths.

If we take these temperature effects of the spectral variation into account, a reconsideration of the identification should be required for some absorption bands which have been recognized as unidentified bands so far, because of the differences in the peak positions and/or peak strengths from the laboratory spectra measured at room temperature. For example, in a comparison between the observational spectrum of NGC 6302 and the low-temperature laboratory spectra, we found that diopside and forsterite are possible candidates of the circumstellar dust of the object.

We wish express our great gratitude to Professor Humihiko Takei and Dr. Shogo Tachibana of Osaka University for synthesizing and supplying high-quality bulk crystals of diopside, forsterite and orthoenstatite. We thank Professor Takao Nakagawa of ISAS for his assistance in operating the spectrometer at ISAS and useful discussions, as well as Mr. Yoshihiko Okamura of ISAS for his handling of the liquid helium and helping to adjust the spectrometer. We would like to thank to Professor Hiroshi Shibai of Nagoya University and Professor Haruyuki Okuda of Gunma Astronomical Observatory for their useful discussions and encouragements. We also thank Professor Dr. L. B. F. M. Waters and Dr. F. J. Molster for kindly permitting us to use the spectrum of NGC 6302 observed by ISO. This work was supported by ISAS and the Research Fellowships of the Japan Society for the Promotion of Science for Young Scientists.

References

Barlow, M. J. 1997, Ap&SS, 255, 315
Beintema, D. A. 1997, Ap&SS, 255, 507
Bowey, J. E., Hofmeister, A. M., Lee, C., Tucker, C., & Ade, P. A. R. 2000, in Proc. The 2nd ISO workshop on analytical spectroscopy: ISO beyond the Peaks, ed. A. Salama, ESA, SP-456, 339
Brandli, G., & Sievers, A. J. 1972, Phys. Rev. B, 5, 3550
Day, K. L. 1976, ApJ, 203, L99
Henning, Th., & Mutschke, H. 1997, A&A, 327, 743
Koike, C., & Shibai, H. 1994, MNRAS, 269, 1011
Koike, C., & Shibai, H. 1998, ISAS Report, No. 671
Koike, C., Tsuchiyama, A., Shibai, H., Suto, H., Tanabé, T., Chihara, H., Sogawa, H., Mouri, H., & Okada, K. 2000, A&A, 363, 1115
Kudo, K. 1996, Fundamentals of Physical Optics (Tokyo: Ohmsha) (in Japanese)
Lim, T., Molster, F. J., Sylvester, R. J., Barlow, M. J., & Waters, L. B. F. M. 1999, A&A, submitted

Malfait, K., Waelkens, C., Bouwman, J., De Koter, A., & Waters, L. B. F. M. 1999, A&A, 345, 181
Malfait, K., Waelkens, C., Waters, L. B. F. M., Vandenbussche, B., Huygen, E., & de Graauw, M. S. 1998, A&A, 332, L25
Mennella, V., Brucato, J. R., Colangeli, L., Palumbo, P., Rotundi, A., & Bussoletti, E. 1998, ApJ, 496, 1058
Molster, F. J. 2000, Ph.D. Thesis, University of Amsterdam, ch. 8
Pottasch, S. R., & Beintema, D. A. 1999, A&A, 347, 975
Smith, R. G., Robinson, G., Hyland, A. R., & Carpenter, G., L. 1994, MNRAS, 271, 481
Tachibana, S. 2000, Ph.D. Thesis, Osaka University, ch. 2
Takei, H., & Kobayashi, T. 1974, J. Crystal Growth, 23, 121
Takei, H., Miura, T., & Morioka, M. 1982, J. Crystal Growth, 60, 453
Tielens, A. G. G. M., & Allamandola, L. J. 1987, in Interstellar Processes, ed. D. J. Hollenbach & H. A. Thronson (Dorderecht: Reidel), 397